

# Effect of atmospheric stability on the wind resource extrapolating models for large capacity wind turbines: A comparative analysis of power law, log law, Deaves and Harris model

<sup>1</sup>Pramod Kumar Sharma, <sup>2</sup>Vilas Warudkar, <sup>3</sup>Siraj Ahmed

<sup>1</sup>Research Scholar, Department of Mechanical Engineering, M.A.N.I.T, Bhopal [M.P] India

<sup>2</sup>Assistant Professor, Department of Mechanical Engineering, M.A.N.I.T, Bhopal [M.P] India

<sup>3</sup>Professor, Department of Mechanical Engineering, M.A.N.I.T, Bhopal [M.P] India

\*Corresponding author: sharma786pramod@gmail.com

Telephone Number : +91 7554051611, +91 7554051616

Fax : +91 7552670562

## Abstract

To observe accurate wind climate from the available met mast measured wind data at different heights an accurate wind shear model is necessary. Since WAsP and windPRO is software package which provides the better representation of wind profile over homogeneous terrain only. Though, a separate module named as WAsP CFD has been added in both of the software to predict correct wind resource in complex terrain also. Nowadays wind resource assessment has been widely dependent on terrain and becomes a key issue for the researchers. It has been found experimentally from earlier work that model of Deaves and Harris shows a better representation of wind profiles on flat terrain at higher heights in comparison to other models such as the PL (power law), the LogL (log law) and the LogLL (Log linear law). This study presents a comparative analysis of three different wind extrapolation models. Based on two year measured wind data from the met mast the at 10 m, 50 m, 80 m, 100 m and 102 m heights, results were compared in different stability classes using Monin-Obukhov similarity theory. The RMSE (root mean square error) and NRMSE (normalized root mean square error) were found to be least in case of log-linear model which is 0.11 and 0.01784 respectively in comparison to the PL and Deaves and Harris models.

**Keywords:** Atmospheric boundary layer, LIDAR, Monin-Obukhov length, Richardson Number, WAsP, windPRO

## Nomenclature

### Abbreviations

WT	Wind turbine
WAsP	Wind resource analysis and application programme
windPRO	Wind energy project design and planning
PL	Power law
LogL	Log-linear law
ABL	Atmospheric Boundary Layer
MOST	Monin-Obukhov similarity theory
LogLL	log-linear law
MLM	Maximum likelihood method
MMLM	Modified maximum likelihood method
Ri	Richardson number
CFD	Computational fluid dynamics
LIDAR	Light detection and ranging
PD	Panofsky and Dutton (PD) model

### Variables

v	wind speed [m/s]
k	shape factor

46	c	size factor [m/s]
47	u*	friction velocity [m/s]
48	z <sub>o</sub>	roughness length [m]
49	K	von Karman's constant (assuming 0.4)
50	L	Monin-Obukhov length [m]
51	ρ	air density [kg/m <sup>3</sup> ]
52	C <sub>p</sub>	specific heat at constant pressure [J/kg.k]
53	H	sensible heat flux [k. m.s <sup>-1</sup> ]
54	T	temperature in Kelvin [k]
55	Φ <sub>m</sub>	Monin-Obukhov stability function
56	α	wind shear exponent
57	v <sub>g</sub>	geostrophic wind speed [m/s]
58	h	atmospheric boundary layer height [m]
59	f	Coriolis parameter [s <sup>-1</sup> ]

60

### 61 **Statistical parameter**

62	n	total number of data
63	m	number of measured data
64	c	number of calculated data
65	μ <sub>m</sub>	$\bar{m}_i$ mean of n measured values
66	σ <sub>m</sub>	standard deviation of n measured values
67	μ <sub>c</sub>	$\bar{c}_i$ mean of n calculated values
68	σ <sub>c</sub>	standard deviation of n calculated values
69	RMSE	root mean square error
70	NRMSE	normalized root mean square error

### 71 **1. Introduction**

72 Accurate measurement of wind resource is necessary to project a wind farm. The earlier method uses cup  
73 anemometer and wind vane to measure the wind velocity and direction. Due to the advancement of wind power  
74 technology attention of researchers had turned to increase the hub height. To measure the wind data at more than  
75 100 m height by using conventional method through met mast is now becoming the costly and time-consuming  
76 process. Henry W. Tieleman 2008 compared the observations from the power law, the logarithmic law and Deaves  
77 and Harris model regarding mean wind speed and turbulence intensity. At 10 m height, nonneutral thermal stability  
78 affects the wind velocity profile and should not be neglected. Daniel R. Drew et al. 2013 observed that Deaves and  
79 Harris wind speed extrapolating model was found to be the best fit at nonequilibrium conditions in urban areas.  
80 Hideki Kikumoto et al. 2017 investigated the accuracy of wind speed measurement using the PL in low-speed  
81 region. The results were compared and analyzed with Doppler Lidar and ultrasonic measured wind data in the urban  
82 boundary layer of Tokyo Japan. Nicholas J. Cook 1997 compared the wind speed profile with the power law and  
83 D&H. The D&H model fitted the profile near the ground and top of the ABL due to satisfying the criteria of both  
84 boundary conditions. Giovanni Gualtieri, Sauro Secci 2011 compared and investigated the accuracy of prediction of  
85 wind speed over a flat and rough region at 10 m and 50 m height above ground level in which the role of  
86 atmospheric stability and surface roughness had discussed. Giovanni Gualtieri 2016 had investigated the time-  
87 varying relation of wind exponent with atmospheric stability. The model was compared with the power law and  
88 found to be the finest and accurate approach regarding wind speed profile and energy yield calculation in neutral  
89 conditions. Some equilibrium wind speed model name as the PL, the LogL and DH had been discussed by  
90 Davenport 1960; Simiu and Scanlan 1996; Deaves and Harris 1978. Panofsky and Dutton 1984 and Elliott 1958  
91 studied the effect of the inner boundary layer with a step change in surface roughness for the wind profile  
92 predictions. Deaves 1981 utilized the concept for heterogeneous terrain in wind speed extrapolating methods.

93 Giovanni Gualtieri 2017 tested and compared the DH model with the PL with all stability conditions. The DH model  
 94 found to be best fitted and tuned, and its accuracy has increased with height from 80 m to 140 m above ground level.  
 95 Due to increasing demand for energy, wind resource prediction has become a crucial issue markedly for energy  
 96 investors to accurately analyze the wind speed at a different hub height of wind turbine. It is essential during the  
 97 feasibility study to abate the cost of wind farm installation. Many researchers worked on different wind  
 98 extrapolating models such as the PL, the LogL, the LogLL, and DH. Every model has its significance and  
 99 assumptions depending on the type of terrain where wind speed has predicted. Sharma et. al. 2014 had optimized  
 100 150 m higher wind monitoring tower using ANSYS. Sharma et. al. 2014 extended earlier work with the  
 101 incorporation of nano and piezoelectric materials in their design.

102

## 103 2. Wind Profile extrapolating models

104 It was the first time when Davenport 1960 originally proposed the PL to design the wind load, especially in  
 105 structural engineering. Due to the simplicity of the PL model which can applied to larger height in compare to the  
 106 logarithmic law subjected to various terrain conditions as per Counihan, 1975. Following models had generally been  
 107 adopted for the wind profile predictions under certain assumptions:

### 108 2.1 Deaves and Harris (D&H) model

109 This model developed in two stages in strong wind conditions. In the first stage, it was developed for the ABL in  
 110 equilibrium over uniform roughness and in the second stage to account for multiple step changes in roughness. The  
 111 model was developed to a different kind of heterogeneous terrain. UK, Australia and New Zealand have adapted this  
 112 model into its wind design codes. If  $u_*$  is the friction velocity,  $k$  is the von Karman constant ( $= 0.4$ ),  $z_o$  is the  
 113 roughness length,  $h$  is atmospheric boundary layer height then velocity  $v$  has been defined as:

114 The D&H model is also known as “logarithmic with parabolic defect” speed profile equation:

$$115 \quad V = \frac{u_*}{k} \left[ \ln \frac{z}{z_o} + 5.75 \left( \frac{z}{h} \right) - 1.88 \left( \frac{z}{h} \right)^2 - 1.33 \left( \frac{z}{h} \right)^3 + 0.25 \left( \frac{z}{h} \right)^4 \right] \quad (1)$$

$$116 \quad h = \frac{u_*}{6f} \quad (2)$$

117 Here,  $f$  is the Coriolis factor which depends on the site latitude angle. The extended model of D&H with a step  
 118 change in roughness had given the concept of transition from the outer and inner boundary layer. It described as:

$$119 \quad u_{*,inner} = u_{*,outer} \left[ 1 - \frac{\ln \left( \frac{z_{o,outer}}{z_{o,inner}} \right)}{0.42 + \ln m_o} \right] \quad (3)$$

$$120 \quad m_o = \frac{0.32 X}{z_{o,inner} (\ln m_o - 1)} \quad (4)$$

121  $X$  is the downward distance towards the change in surface roughness, and  $m_o$  is the constant parameter.

122

123 As per similarity theory,

$$124 \quad \frac{V}{u_*} \cong \frac{1}{k} \ln \left( \frac{z}{z_o} \right) \text{ when } z \cong h \quad (5)$$

$$125 \quad V \rightarrow V_G \text{ and } \frac{dV}{dz} \rightarrow 0 \text{ as } z \rightarrow h \quad (6)$$

126  $V_G$  stands for the geostrophic wind speed satisfies the criteria of upper and lower boundary conditions to the ABL.

127 Geostrophic wind speed calculated when the thermal flux generated by the heat and friction are equal.

## 128 2.2 Log- Law model

129 The log law model derived from Eq. (5) and holds over a ground surface:

$$130 \quad V = \frac{u_*}{k} \ln\left(\frac{z}{z_0}\right) \quad (7)$$

131 It is clear from Eq. (7) That log law satisfies the lower boundary conditions only not the upper one. Typically, it  
132 found that the power law does not fit well at the higher height ranger (typically more than 150 m).

## 133 2.3 Power law model

134 The wind speed at a height z uses the empirical formula:

$$135 \quad \frac{V}{V_{ref}} = \left(\frac{z}{z_{ref}}\right)^\alpha \quad (8)$$

136 Here,  $V_{ref}$  refers to the wind speed at the height say  $z_{ref}$ . The Power law indicates the increment of surface wind  
137 speed concerning height z. The PL neither satisfies the upper boundary nor the lower boundary conditions. In  
138 comparison to log law model, it fits well with the wind speed profile at larger height, which is one of the critical  
139 reason for its preference. Though, it had not been recommended to use it very close to the ground. Most of the  
140 research matched well with the PL over the height value from 30 m to 300 m a.g.l. The value of  $\alpha$  varies concerning  
141 wind speed, height and surface roughness. In practice, the wind shear exponent  $\alpha$  often assumed as equivalent to the  
142 aerodynamic roughness length  $z_0$ .

## 143 2.4 Estimation of Monin-Obukhov length

144 Monin defines the turbulence within the surface boundary layer- Obukhov length scale L as:

$$145 \quad L = - \frac{\rho C_p T u_*^3}{k.g.H} \quad (9)$$

146 Where  $\rho$  stands for air density at temperature T,  $C_p$  is the specific heat at constant pressure, k is the Von Karman  
147 constant  $u_*$  is the friction velocity, and H is the sensible heat flux. The Monin- Obukhov length scale L can calculate  
148 by computing the Bulk Richardson number which requires only single wind speed and temperature measurements at  
149 two heights. Gradient and bulk Richardson number defined as:

$$150 \quad R_i = \frac{g \Delta z \Delta \theta}{\theta_1 \Delta u^2} \quad (10)$$

151 Where  $\Delta \theta = \theta_2 - \theta_1$ ,  $\Delta z = z_2 - z_1$  and  $\Delta u = u_2 - u_1$  are the measured parameter at two height. When the temp. and wind  
152 speed measurement is available only a single height (Barker and Baxter, 1975)

$$153 \quad R_{ib} = \frac{g z_2 \Delta \theta}{\theta_2 u_2^2} \quad (11)$$

$$154 \quad \varepsilon = \frac{\varphi_m^2}{\varphi_h} R_i \text{ (Businger et.al., 1971) suggested} \quad (12)$$

155  $\frac{\bar{z}}{L} = \varepsilon$ ,  $\bar{z}$  stands for the geometrical mean height of  $z_1$  and  $z_2$ , and  $\varphi_m$  and  $\varphi_h$  are the nondimensional functions related to  
156 Wind shear and temperature gradient, as per (Dyer, 1974)  $\varphi_m$  and  $\varphi_h$  :

$$157 \quad \varphi_m = \begin{cases} (1 - \gamma \varepsilon)^{\frac{1}{4}}, & \varepsilon < 0 \\ (1 + \beta \gamma), & \varepsilon \geq 0 \end{cases} \quad (13)$$

$$158 \quad \varphi_h = \begin{cases} R(1 - \gamma \varepsilon)^{\frac{1}{2}}, & \varepsilon < 0 \\ (R + \beta \gamma), & \varepsilon \geq 0 \end{cases} \quad (14)$$

159 (Binkowski, 1975) found the following results, the function based on two stability conditions

$$\varepsilon = \begin{cases} \frac{R_i}{R} (1 - \gamma R_i)^{\frac{1}{2}} / (1 - \gamma' R_i)^{\frac{1}{2}} & R_i \leq 0 \\ \frac{R_i}{R} \frac{1}{1 + \frac{R_i \beta^2}{\beta}} & 0 < \frac{R_i \beta^2}{\beta} < 1 \end{cases} \quad (15)$$

$$\bar{z} = \frac{z_1 + z_2}{2}, \quad \bar{z} \text{ is the mean height} \quad (16)$$

$$\frac{z_2}{L} = \frac{k R_{ib} F^2}{G} \quad (17)$$

$$F = \frac{u}{u_*} \begin{cases} \ln \left[ \left( \frac{z_2}{z_0} \right) \left( \frac{\eta_o^2 + 1}{\eta_2^2 + 1} \right) \left( \frac{\eta_o + 1}{\eta_2 + 1} \right)^2 \right] + 2 \tan^{-1} \left( \frac{\eta_o - \eta_2}{1 + \eta_o \eta_2} \right), & L \leq 0 \\ \ln \left( \frac{z_2}{z_0} \right) + \frac{\beta z_2}{L}, & L \geq 0 \end{cases} \quad (18)$$

L depends upon two stability conditions

$$G = \frac{\Delta \theta u_*}{(-w'\theta')} = \begin{cases} R \ln \left[ \left( \frac{z_2}{z_0} \right) \left( \frac{\lambda_1 + 1}{\lambda_2 + 1} \right)^2 \right], & L \leq 0 \\ R \left[ \ln \left( \frac{z_2}{z_0} \right) + \frac{\beta (z_2 - z_1)}{L} \right], & L \geq 0 \end{cases} \quad (19)$$

$$\eta_2 = (1 - \gamma z_2 / L)^{\frac{1}{4}} \quad (20)$$

$$\eta_o = (1 - \gamma z_o / L)^{\frac{1}{4}} \quad (21)$$

$$\lambda_1 = (1 - \gamma' z_1 / L)^{\frac{1}{2}} \quad (22)$$

$$\lambda_2 = (1 - \gamma' z_2 / L)^{\frac{1}{2}} \quad (23)$$

Where  $\eta_2$ ,  $\eta_o$ ,  $\lambda_1$ ,  $\lambda_2$  are the function of Monin- Obukhov length L. G is the function of Ri and mean gradient height z. F stands for the logarithmic function of speed and friction velocity.

174

### 175 3. Observation and site details

176 Jamgodrani hills have a huge potential regarding power production. The 100 m mast located in District Dewas at  
 177 Jamgodrani Hills. The elevation of the mast location is 573m above mean sea level. Site coordinate has been  
 178 converted into UTM (Universe Transverse Mercator) system to perform line and area roughness calculation purpose  
 179 using WAsP and windPRO. There were five wind anemometers, and wind vane had mounted on the mast to  
 180 measure wind speed and direction respectively. To verify the Monin- Obukhov Similarity theory two temperatures  
 181 and one pressure sensor had also installed. Table 1 and Fig.1 shows the mast details and location respectively.

182 Table 1 Site Details

Site Coordinate	(E)Longitude- 76°09'2.50" (N) Latitude- 22°58' 58.20" UTM-2542426 N, 619480 E
Duration	2015 to 2017
Site name	Jamgodrani Hills
District	Dewas
State name	Madhya Pradesh
Mast Height	100m
Elevation	573mAMSL
Location of Anemometer	10m, 25m, 50m, 80m, 100m.
Location of Wind vane	10m, 25m, 50m, 80m, 100m
Location of Pressure sensors	2m, 10m
Location of temperature sensors	2m, 10m

183



184

Fig. 1 Met mast location (The point shows the met mast location, Source Google Earth)

185

186

187

188

189

190

191

Weibull parameter (k and c) calculated by two different methods namely as MLM and MMLM. It is very much clear from the Table 3 in comparison to Table 2 Weibull parameter are more than Table 2. Experimentally, it found that the Weibull parameters calculated by the MMLM provides more accurate results in comparison to MLM.

MLM is a widely accepted method to estimate the Weibull parameter. It required a more extensive tool for mathematical calculations. In the first step, k calculated by using the following equation.

$$k = \left( \frac{\sum_{i=1}^n v_i^k \ln(v_i)}{\sum_{i=1}^n v_i^k} - \frac{\sum_{i=1}^n \ln(v_i)}{n} \right)^{-1} \quad (24)$$

$$c = \left( \frac{1}{n} \sum_{i=1}^n v_i^k \right)^{\frac{1}{k}} \quad (25)$$

n stands no of observation of zero wind speed and  $v_i$   $i_{th}$  operation wind speed.

195

196

197

198

This method is similar to MLM and estimated by iteratively using the following two equations. It used when wind data is available in frequency distribution form. If  $v_i$  is the wind speed related to bin i,  $f(v_i)$  is the frequency range within the region of bin I, n is the total no of bins and  $f(v \geq 0)$  is the probability of wind speed.

$$k = \left( \frac{\sum_{i=1}^n v_i^k \ln(v_i) f(v_i)}{\sum_{i=1}^n v_i^k f(v_i)} - \frac{\sum_{i=1}^n \ln(v_i)}{f(v \geq 0)} \right)^{-1} \quad (26)$$

$$c = \left( \frac{1}{f(v \geq 0)} \sum_{i=1}^n v_i^k \right)^{\frac{1}{k}} \quad (27)$$

Table 2 Weibull parameter by MLM

100m		80m		50m		10m	
k	c	k	c	k	c	k	c
2.24	7.131	2.219	6.70	2.3621	6.25	2.164	4.193

202

203

204 Table 3 Weibull parameter by MMLM

100m		80m		50m		10m	
k	c	k	c	k	c	k	c
2.431	7.67	2.42	7.24	2.57	6.78	2.45	4.736

205 \*Roughness length=0.3183m, \*Class= 2.8

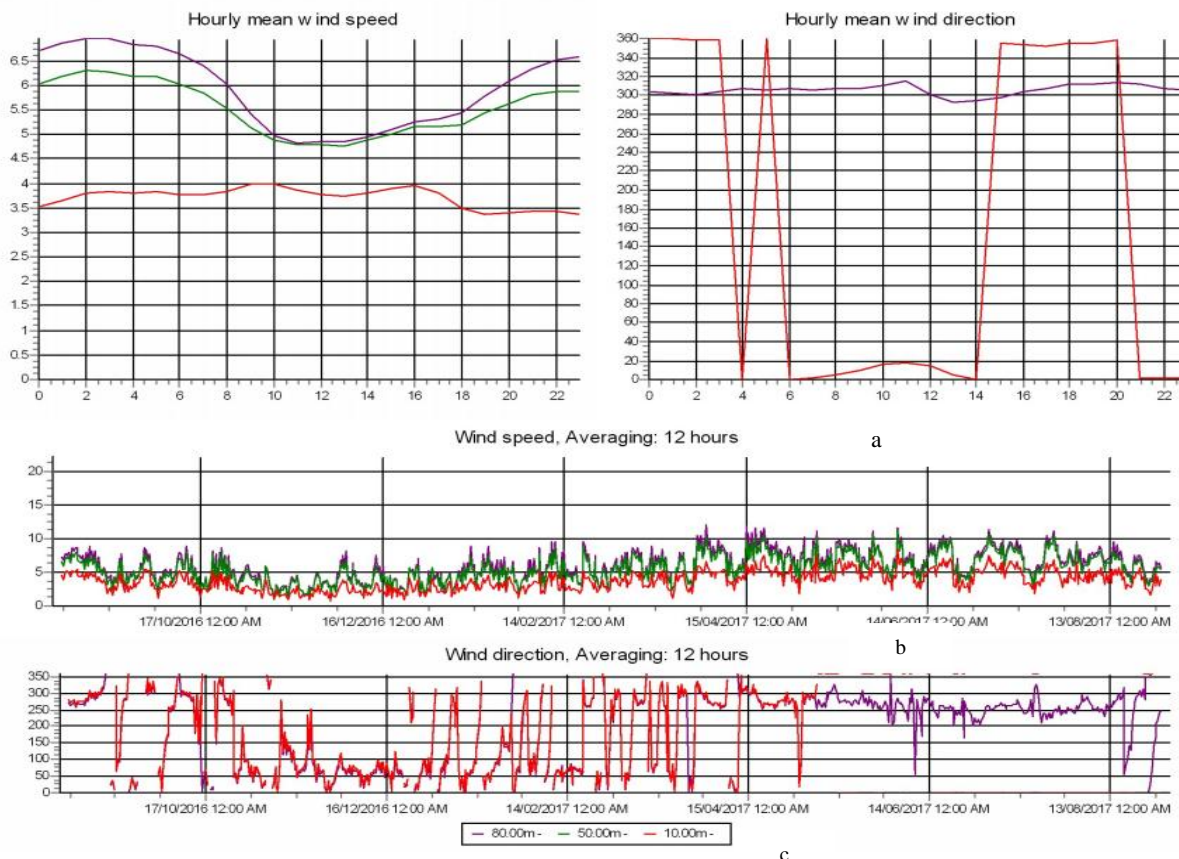
206 **4. Result & Discussion**

207 Annual mean wind speed and mean turbulence intensity calculated at different heights from ground level. It is clear  
 208 from Table 4 that the annual wind speed increase concerning height, but mean turbulence intensity decreases. Due to  
 209 more predominate viscous and obstruction effect near the ground level wind turbulence is more. Turbulence  
 210 intensity seems to decrease with the height due to a decrease in surface shear stress.

211 Table 4 Wind characteristics

AMWS (Annual Mean wind speed) in m/s				Mean turbulence intensity (TU)			
100 m	80 m	50 m	10 m	100 m	80 m	50 m	10 m
6.32	5.93	5.53	3.71	0.124	0.143	0.150	0.24

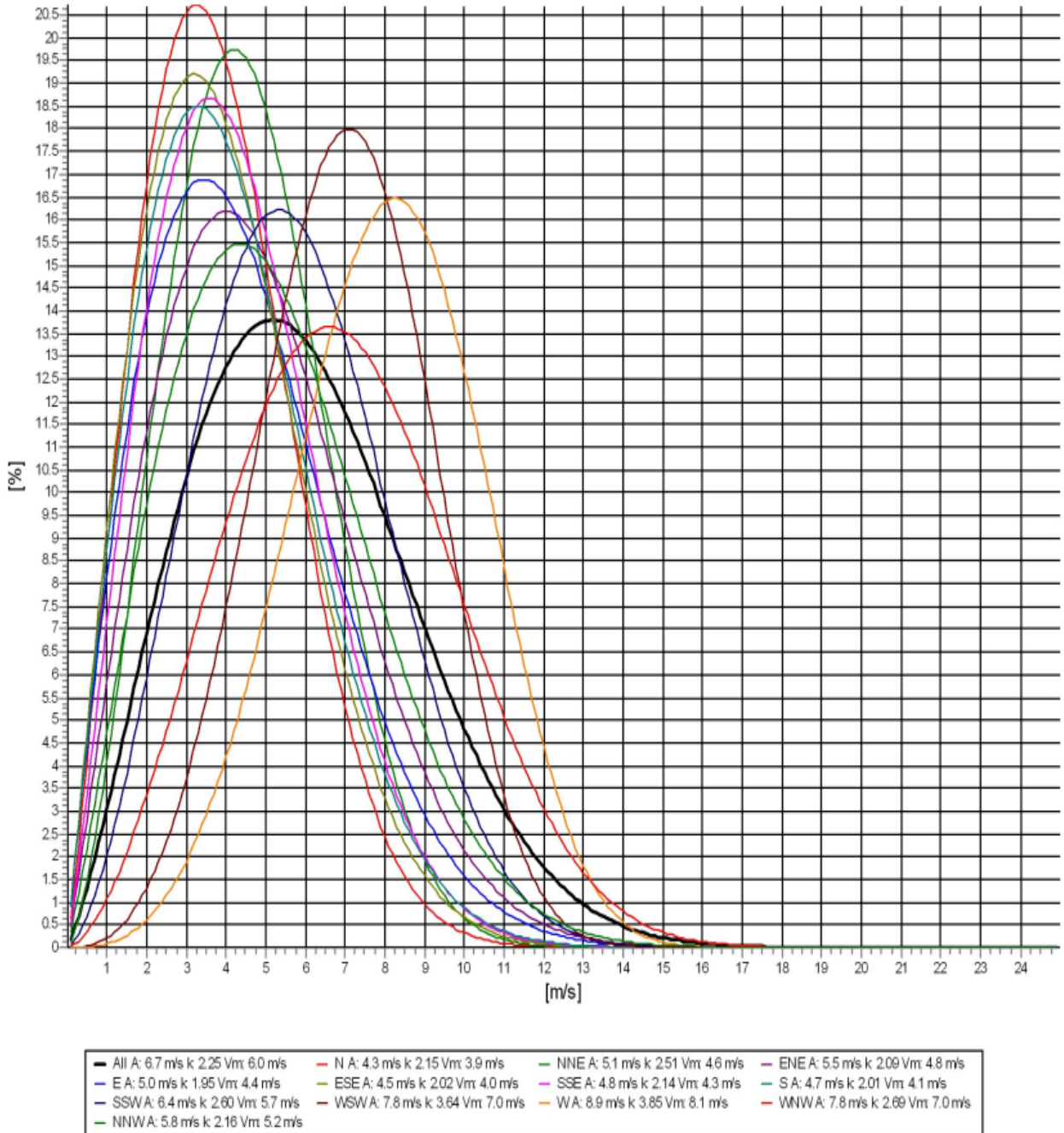
212



213

214 Fig. 2 Wind speed and direction variation (Source: windPRO 3.1) (a): Variation of hourly wind speed in m/s and  
 215 Direction in degree, (b): average wind direction, (c): wind direction at 50 m, 80 m, and 100 m heights.

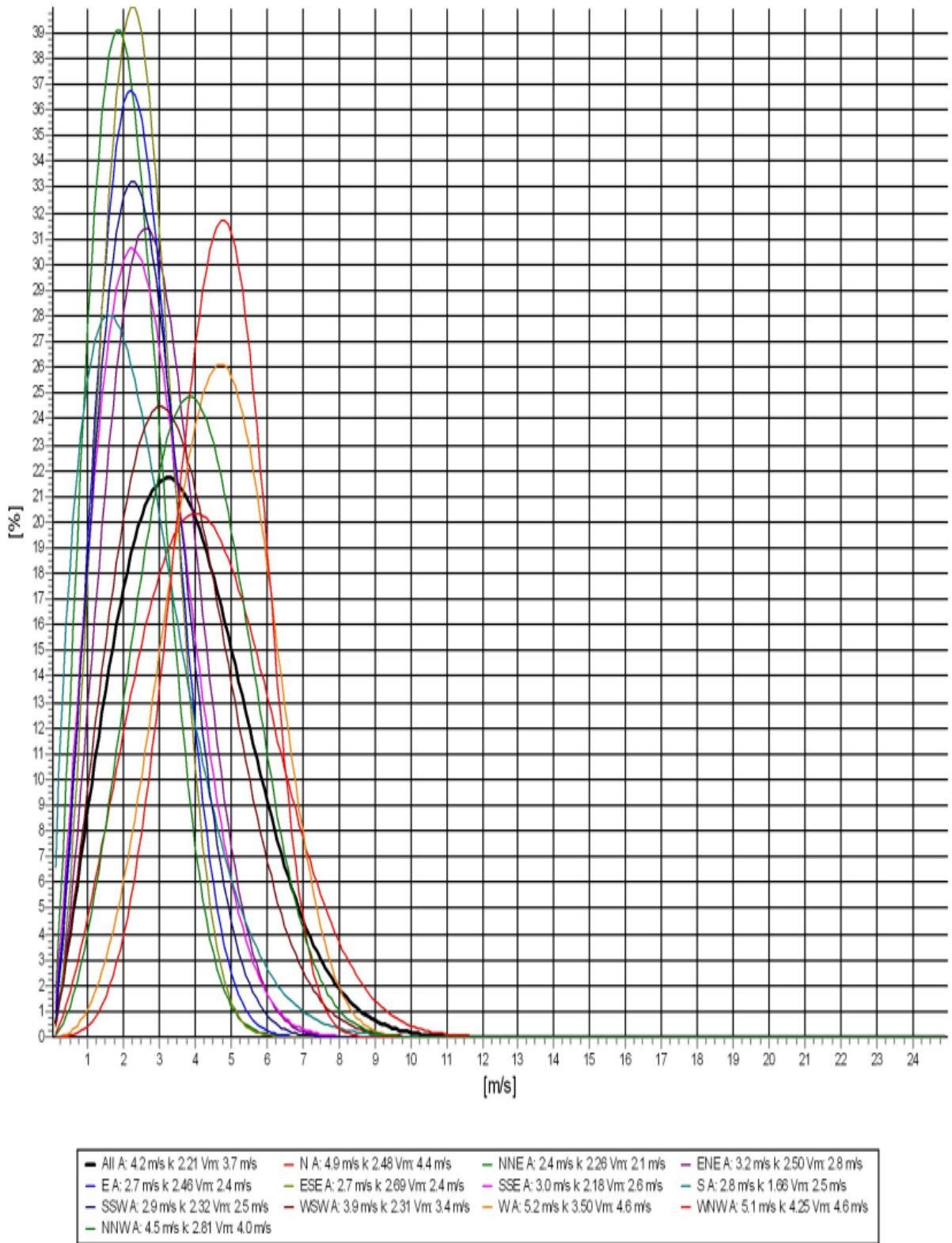
216 The hourly variation of wind speed and direction has been shown in Fig. 2 at 10 m, 50 m, and 80 m height  
 217 respectively. Blue shown in Fig. 2 signifies the wind speed and direction at 100 m hub heights. Weibull parameters  
 218 have been divided into 12 sectors with the given direction and typically illustrated in Fig.3 and Fig. 4 respectively at  
 219 80 m and 10 m height respectively.



220

221

Fig. 3 Sector-wise Weibull parameter distribution at 80m height a.g.l. (Source: windPRO 3.1)



222

223

Fig. 4 Sector wise Weibull parameter distribution at 10m height a.g.l. (Source: windPRO 3.1)

224 Fig.3 and Fig. 4 shows the sector-wise distribution of Weibull parameter at 80m and 10m height respectively.

225

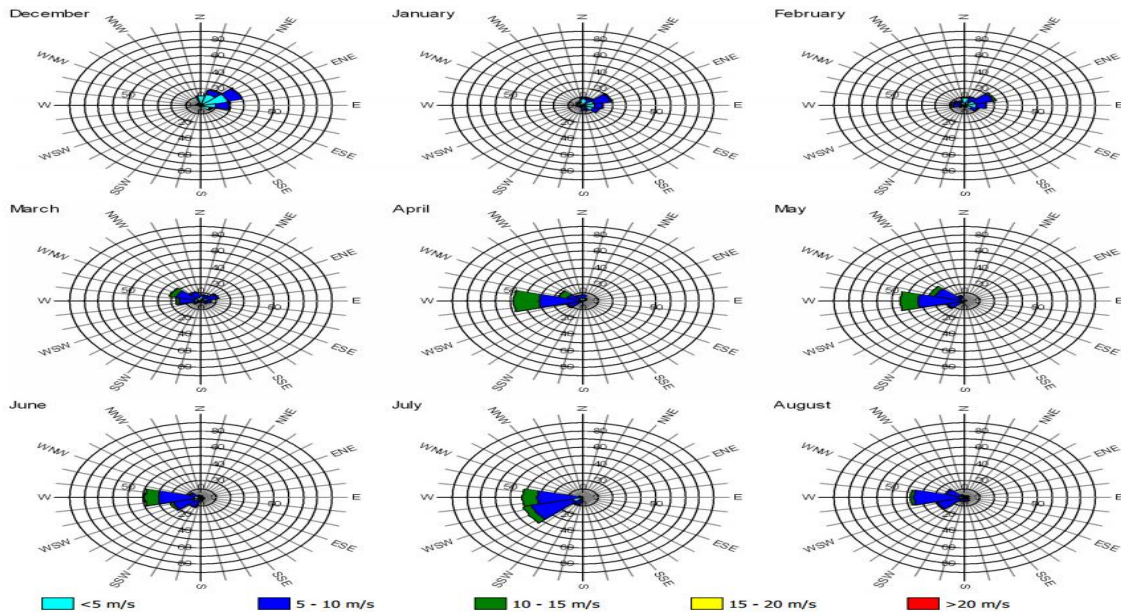


Fig. 5 Energy rose at 80m height (Source: windPRO 3.1)

229

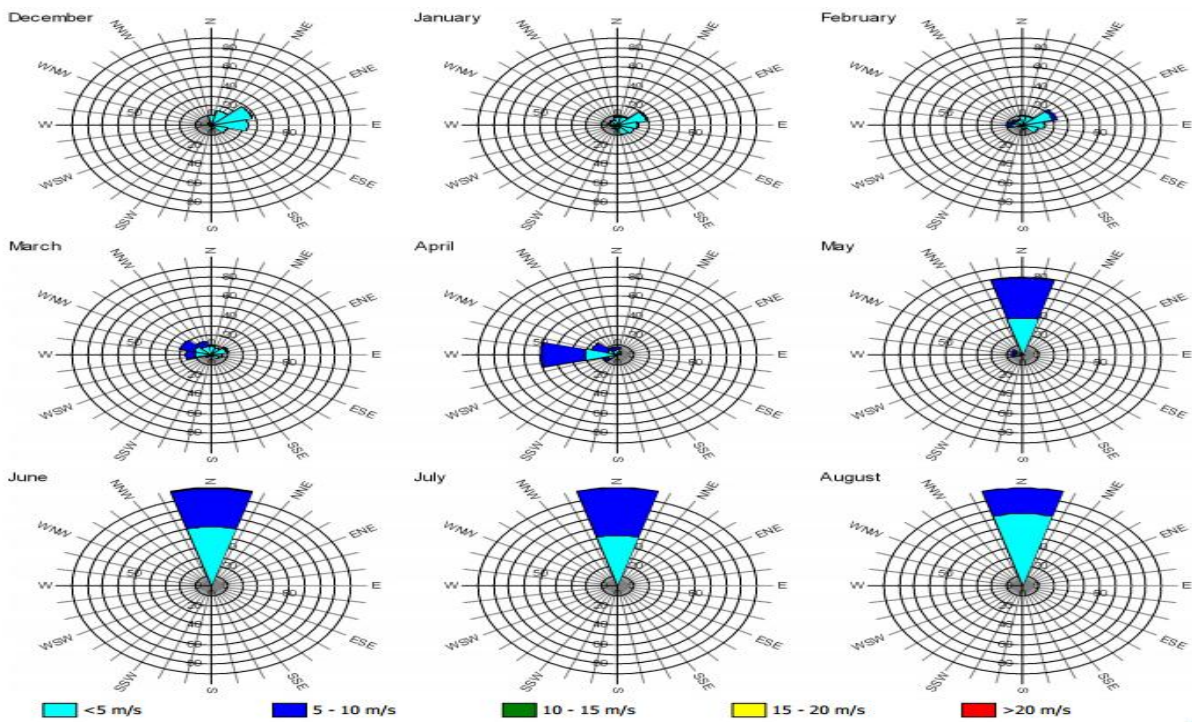
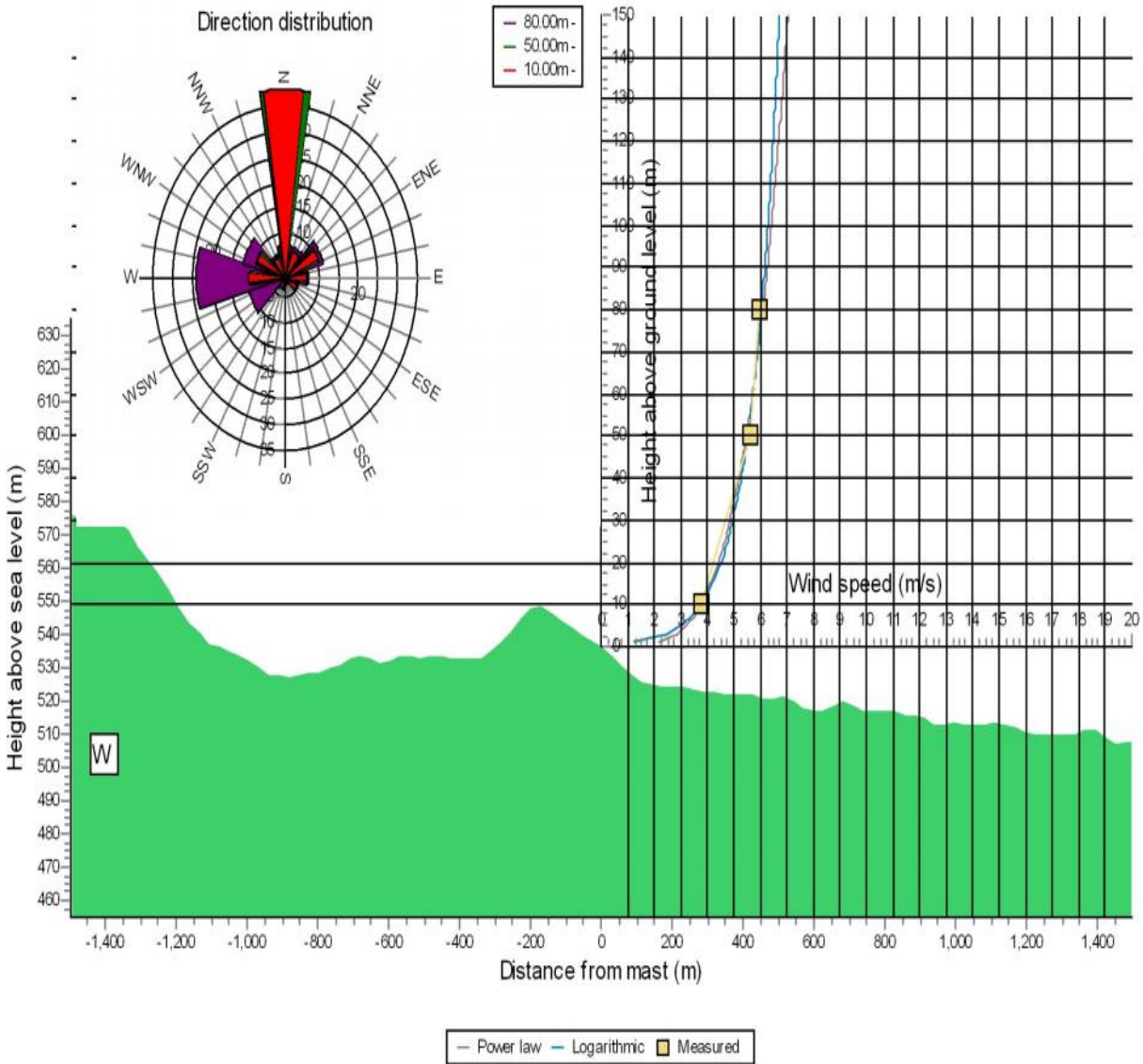


Fig. 6 Energy rose at 10m height (Source: windPRO 3.1)

231 In Fig. 5 (April month) up to 20m/s wind speed shown, which produces maximum power density at 80m height.  
 232 While Fig. 6 indicates that the maximum wind speed can be utilized for the power production is 3 -5 m/s at 10m  
 233 height. The measured wind speed at 10m a.g.l. can be taken for reference purpose. Further Wind speed has been  
 234 extrapolated using the PL from 50m to 100m and 80m to 100m by  $\alpha_{10-50} = 0.2483$  and  $\alpha_{50-80} = 0.1474$  respectively.  
 235 By taking the surface length of  $z_0$  0.3183m, von Karman factor 0.4 and friction velocity  $u_*$  0.4316 m/s the wind  
 236 speed can be found using the LogL at 100m a.g.l as 6.20m/s.

237 The Monin- Obukhov Length similarity had applied at Jamogadrani hills which predict that the atmosphere is  
 238 strongly stable and wind speed using D&H model found to be 6.68m/s. The Richardson Number is 0.35614 which  
 239 has been used to calculate Monin- Obukhov scale.

240



241

242 Fig. 7 Mean wind profile using power law and LogL respectively

243 Table 5 Comparative analysis of different models  
 244

Parameter/Results	Predicted by PL ( $\alpha_{10-50} = 0.2483$ )	Predicted by PL ( $\alpha_{50-80} = 0.1474$ )	LogL	D&H model
Wind speed in m/s	6.580	6.135	6.204	6.681
RMSE	0.26398	0.18085	0.111701	0.36485
NRMSE	0.04094	0.02905	0.017842	0.056139

245  
 246 It is clear from Table 5 that Log law fitted and best matches the wind profile. RMSE and NRMSE found to be least  
 247 in case of Log law in compare to PL and D&H model. The actual measured wind speed by wind anemometer is 6.32  
 248 m/s at 100m a.g.l. It can see from Fig. Seven that the accuracy of the LogL increases from the height above 80m  
 249 a.g.l.

250 **5. Conclusion**

251 To validate its reliability for addressing MW WTs, the PL, LogL and D&H model assessed at hub heights at 10 m,  
 252 50 m, 80 m and 100 m. Based on a two-year wind data of 10 min. Observations including temperature and pressure  
 253 data from the met mast of Jamdani hills, all models were compared. The application of models required prior  
 254 assessment of sites surface parameter such as  $\alpha$  for power law, friction velocity and surface length for Log law and  
 255 Coriolis factor, ABL height for D&H model. Though D&H model developed for strong wind conditions subjected to  
 256 neutral conditions; it forced to apply for all stability regions.

257 The RMSE and NRMSE were found to be at least for the PL, the LogL, Deaves and Harris model up to height 80m  
 258 a.g.l. Within the extrapolating range. The result seems to the LogL capability of best producing at a higher level.  
 259 This model was found suitable for strong adiabatic conditions. However, the overall accuracy of LogL model during  
 260 these conditions should choose as a model's key factor. Practically, in Indian conditions the DH model could not fit  
 261 appropriate due to two limitations: i) reliable friction observation ii) accurate site's surface length assessment. The  
 262 value of  $Z_0$  has the major effect on DH model.

263 Based on 10 min. Wind speed, pressure and temperature data the minimum RMSE and NRMSE found to be 0.11  
 264 and 0.01 respectively. The PL exhibited the more accuracy across all extrapolations ranges and for all stability criteria,  
 265 which is used particularly in predicting wind speed profile variation. Currently, obtained results strongly encourage  
 266 further uses of the PL, which would deem as a future research topic from a wind energy scenario. At Jamgodrani  
 267 hills, the LogL proved to be the finest in the prediction of the extrapolated wind speed, thus supporting its validity  
 268 over the entire ABL.

269 **References**

270 Barker, E. H., Baxter, T. L., 1975. A note on the computation of atmospheric surface layer fluxes for use in  
 271 numerical modeling. *J. Appl. Met.* 14, 620-622.  
 272 Binkowski, F. S. 1975. On the empirical relationship between the Richardson number and the Monin-Obukhov  
 273 stability parameter. *Atmospheric Environmental*, 9, 453-454.  
 274 Businger, J. A., Wyngaard J. C, Izumi Y. and Bradley E. F. 1971. Flux- profile relationships in the atmospheric  
 275 surface layer. *J. Atmos. Sci.* 288, 181-189.  
 276 Cook, Nicholas J., 1997. The Deaves and Harris ABL model applied to the heterogeneous terrain. *Journal of Wind  
 277 Engineering and Industrial Aerodynamics.* 66 (1991) 197-214.  
 278 Counihan, J., 1975. Adiabatic atmospheric boundary layers: a review and analysis of data from the period 1880-  
 279 1972. *Atmos. Environ.* 9, 871-905. [http://dx.doi.org/10.1016/0004-6981\(75\)90088-8](http://dx.doi.org/10.1016/0004-6981(75)90088-8).  
 280 Davenport, A., 1960. The rationale for determining design wind velocities. *Journal of Structural Engineering, ASCE*  
 281 86,39-68.

282 Deaves, D.,1981.Computation of wind flow over changes in surface roughness. *Journal of Wind Engineering and*  
283 *Industrial Aerodynamics* 7, 65–94.

284 Deaves, D., Harris, R.,1978.A Mathematical model of the structure of strong winds. Report76. Construction Industry  
285 Research and Information Association.

286 Drew, Daniel R., Barlow, Janet F., Lane, Siân E., 2013. Observations of wind speed profiles over Greater London,  
287 UK, using a Doppler lidar. *J. Wind Eng. Ind. Aerodyn.* 121(2013)98–105.

288 Dyer, A., 1974. A review of flux-profile relationships. *Boundary-Layer Met.* 7, 363-312.

289 Elliott, W.,1958. The growth of the atmospheric internal boundary layer. *American GeophysicalUnion*39,1048–  
290 1054.

291 Gualtieri, Giovanni., Secci, Sauro ., 2011. Comparing methods to calculate atmospheric stability-dependent wind  
292 speed profiles: A case study on coastal location. *Renewable Energy* 36 (2011) 2189-2204

293 Gualtieri, Giovanni., 2017. Wind resource extrapolating tools for modern multi-MW wind turbines: Comparison of  
294 the Deaves and Harris model vs. the power law. *Journal of Wind Engineering & Industrial Aerodynamics* 170  
295 (2017) 107–117.

296 Gualtieri, Giovanni., 2016. Atmospheric stability varying wind shear coefficients to improve wind resource  
297 extrapolation: A temporal analysis. *Renewable Energy* 87 (2016) 376-390.

298 Kikumoto, Hideki., Ooka, Ryoza., Sugawara, Hirofumi., Lim, Jongyeon., 2017. An observational study of  
299 power-law approximation of wind profiles within an urban boundary layer for various wind conditions. *Journal of*  
300 *Wind Engineering & Industrial Aerodynamics* 164 (2017) 13–21.

301 Panofsky, H., Dutton, J., 1984. *Atmospheric Turbulence: Models and Methods for Engineering Applications*. Wiley.

302 Simiu, E., Scanlan, R.,1996.*Wind effects on structures fundamentals and applications to design*. John Wiley and  
303 Sons Inc.

304 Sharma, Pramod Kumar., Baredar, Prashant V. 2017. Analysis of the piezoelectric energy harvesting small-scale  
305 device – a review. <https://doi.org/10.1016/j.jksus.2017.11.002>.

306 Sharma, Pramod Kumar., Warudkar, Vilas., Ahmed, Siraj. 2014. Experimental investigation of Al 6061/ Al2O3  
307 Composite and Analysis of its mechanical properties on onshore wind tower using the hybrid technique for Indian  
308 Condition. *Procedia Materials Science* 5 (2014 ) 147 – 153.

309 Sharma et al., 2014. A Review on Electromagnetic Forming Process.” *Procedia Materials Science* 6 ( 2014 ) 520 –  
310 527.

311 Sharma, Pramod Kumar., Warudkar, Vilas., Ahmed, Siraj. 2014. Design and Optimization of 150 m Higher Wind  
312 Monitoring Tower (Indian Condition). *International Journal of Scientific Engineering and Technology*. (ISSN:  
313 2277-1581). 2014 Volume No.3 Issue No.2, pp : 85 – 89.

314 Tieleman, Henry W., 2008. Strong wind observations in the atmospheric surface layer. *Journal of Wind Engineering*  
315 *and Industrial Aerodynamics* 96 (2008) 41–77.

316

317

318

319

320

321

322

323